ACS OMEGA

http://pubs.acs.org/journal/acsodf

Article

# Novel Mitochondria-Targeting and Naphthalimide-based Fluorescent Probe for Detecting HClO in Living Cells

Junhong Xu, Chunyan Wang, Qiujuan Ma,* Hongtao Zhang,* Meiju Tian, Jingguo Sun, Baiyan Wang,* and Yacong Chen

Cite This: *ACS Omega* 2021, 6, 14399−14409

Read Online

ACCESS | Metrics & More | Article Recommendations | Supporting Information

**ABSTRACT:** As a key reactive oxygen species (ROS), hypochlorous acid (HClO) plays an important role in many physiological and pathological processes. The mitochondria-targeting probes for the highly sensitive detection of HClO are desirable. In present work, we designed and synthesized an original mitochondria-localizing and turn-on fluorescent probe for detecting HClO. 4-Aminonaphthalimide was employed as the fluorescent section, the (2-aminoethyl)-thiourea unit was utilized as a typical sensing unit, and the quaternized pyridinium moiety was used as a mitochondria-targeted localization group. When HClO was absent, the probe showed weak fluorescence. In the existence of HClO, the probe revealed a blue fluorescence. Moreover, the turn-on fluorescent probe was able to function in a broad pH scope. There was an excellent linearity between the fluorescence emission intensity at 488 nm and the concentrations of HClO in the range of $5.0 \times 10^{-7}$ to $2.5 \times 10^{-6}$ mol·L$^{-1}$. Additionally, the probe had almost no cell toxicity and possessed an excellent mitochondria-localizing capability. Furthermore, the probe was able to image HClO in mitochondria of living PC-12 cells. The above remarkable properties illustrated that the probe was able to determine HClO in mitochondria of living cells.

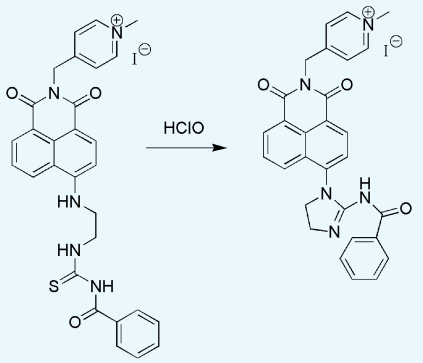


## INTRODUCTION

Reactive oxygen species (ROS), including superoxide ($O_2^{\bullet-}$), hydrogen peroxide($H_2O_2$), hypochlorous acid or hypochlorite (HClO/$ClO^-$), and hydroxyl radicals ($^\bullet$OH), are important oxygen-containing species, which exert a strong influence in many physiological and pathological processes, such as senescence and immune regulation.[1,2] In different ROS, endogenous HClO is mainly yielded by the reaction of $H_2O_2$ and $Cl^-$ through myeloperoxidase (MPO) as a catalyst. HClO is an unstable weak acid, which is partially dissociated into $ClO^-$ under physiological conditions.[3,4] As a bactericidal medium in the process of human immune defense, HClO/$ClO^-$ can kill harmful bacteria and pathogens.[5−7] However, excessive or disordered intracellular HClO levels may lead to lung injury, arteriosclerosis, rheumatoid arthritis, kidney damage, and even some cancers.[8−12] Mitochondria provide energy for cell activities, are the main site of aerobic respiration, and are the most active organelles for oxidative phosphorylation and electron transport.[13−15] It has been reported that most of the ROS in cells come from mitochondria.[16,17] HClO is responsible for cell signal transmission and maintaining normal cell function. The level of intracellular HClO is interrelated with the oxidation−reduction balance occurring in mitochondria, which is very important for retaining the normal role of mitochondria. Therefore, it is of great biomedical significance to accurately detect the changes of the content of HClO in mitochondria for studying the relationship between the biological processes related to HClO and human diseases.

Compared with other methods, such as colorimetric method,[18] electrochemical analysis,[19,20] atmospheric pressure ionization mass spectrometry,[21] liquid chromatography electrospray ionization mass spectrometry,[22] and ion chromatography,[23] fluorescence analysis has been widely used in the detection of HClO due to its obvious advantages such as simple, high sensitivity and easy to realize on-line detection.[24−32] In recent years, bifunctional mitochondrial fluorescent probes, which can not only locate in mitochondria but also detect various active species in mitochondria, have become a research hotspot. It is reported that some of the fluorescent probes have been reported for quantitatively detecting active oxygen species in mitochondria, such as $H_2O_2$,[33−35] $O_2^{\bullet-}$,[36] and $^\bullet$OH,[37,38] but there are few reports on the high-efficiency detection of mitochondrial HClO.[39−43] Therefore, it is urgent to design fluorescent probes that can detect the changes in HClO content in mitochondria rapidly.

**Received:** March 9, 2021
**Accepted:** May 14, 2021
**Published:** May 26, 2021

**Scheme 1. Preparation of Fluorescent Probe 1: (a) Tetrahydrofuran, 4-Pyridinemethaneamine, Room Temperature, 6 h, 79%; (b) Ethylene Glycol Monomethyl Ether, Ethylenediamine, Reflux, 4 h, 60%; (c) Anhydrous Dichloromethane, Benzoyl Isothiocyanate, Room Temperature, 6 h, 47%; (d) Toluene, Methyl Iodide, Room Temperature, 2 h; Reflux, 3 h, 31%**

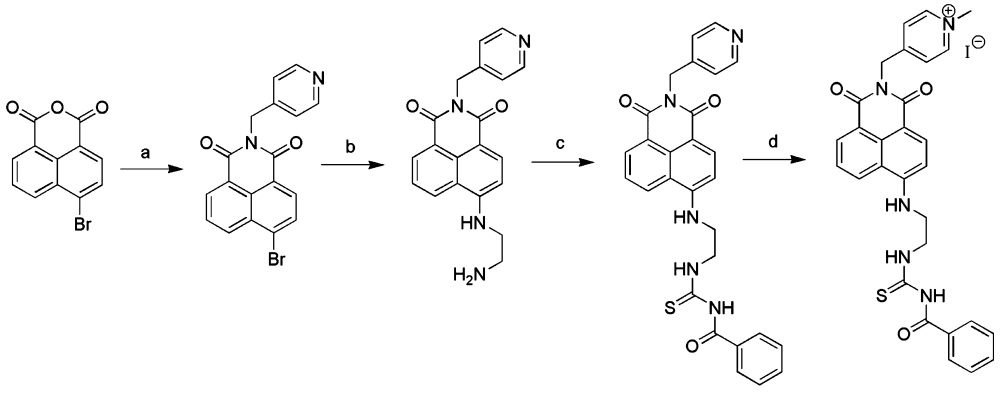


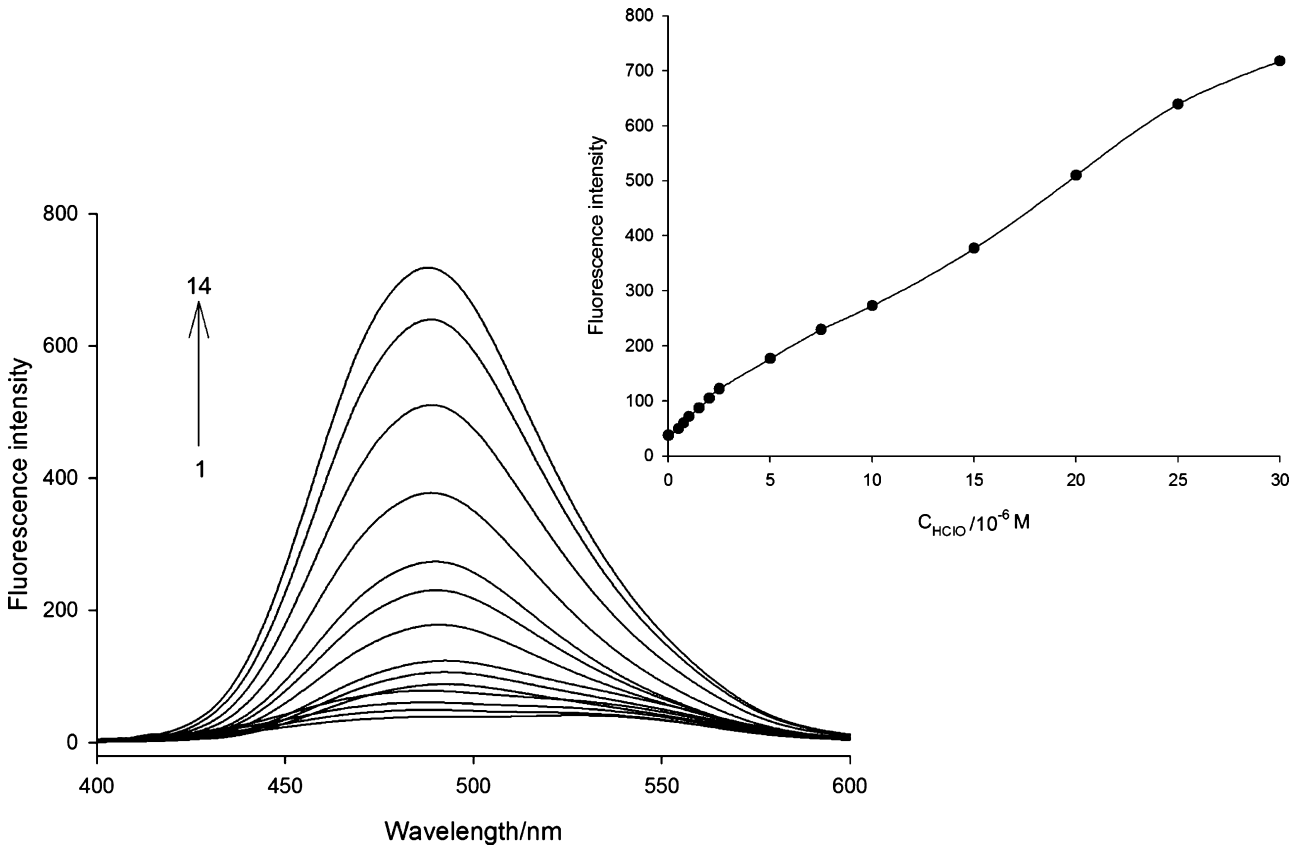


**Figure 1.** Fluorescence spectra of probe **1** (7.5 $\mu$M) in presence of different concentrations of HClO: 0, 0.50, 0.75, 1.0, 1.5, 2.0, 2.5, 5.0, 7.5, 10, 15, 20, 25, and 30 $\mu$M from 1 to 14 excited at 370 nm. Inset: The variation of fluorescence intensity of probe **1** (7.5 $\mu$M) in the presence of different concentrations of HClO from 0 to 30 $\mu$M.

In the present paper, we developed a novel mitochondria-targeted single wavelength-enhanced fluorescent probe **1** (Scheme 1), which had been magnificently utilized to detect HClO in living cells. Based on the membrane potential of mitochondria with −180 mV, quaternized pyridinium moiety with positive charge was used to dye mitochondria.[44,45] Classical 4-aminonaphthalimide was used as the fluorescent unit on the basis of its superior internal charge transfer (ICT) structure and attractive photophysical characteristics.[40,41] Because sulfur atom with powerful electron-donating properties was able to react with HClO,[46] the (2-aminoethyl)-thiourea group was chosen as the specific sensing group of HClO. When HClO is absent, the fluorescence emission of the probe was weak. After interaction with HClO, the probe emitted remarkable blue fluorescence with a 19-times enhancement. The change of fluorescence signal is an important basis for the detection of HClO. The testing results showed that the probe demonstrated high sensitivity, wide pH range (2.00−11.00), high selectivity over other ROS, reactive nitrogen species (RNS) and some metal ions, and fast response (around 60 s). The PC-12 cell imaging experiment verified that the probe is applicable for imaging HClO in mitochondria.


https://doi.org/10.1021/acsomega.1c01271
ACS Omega 2021, 6, 14399−14409

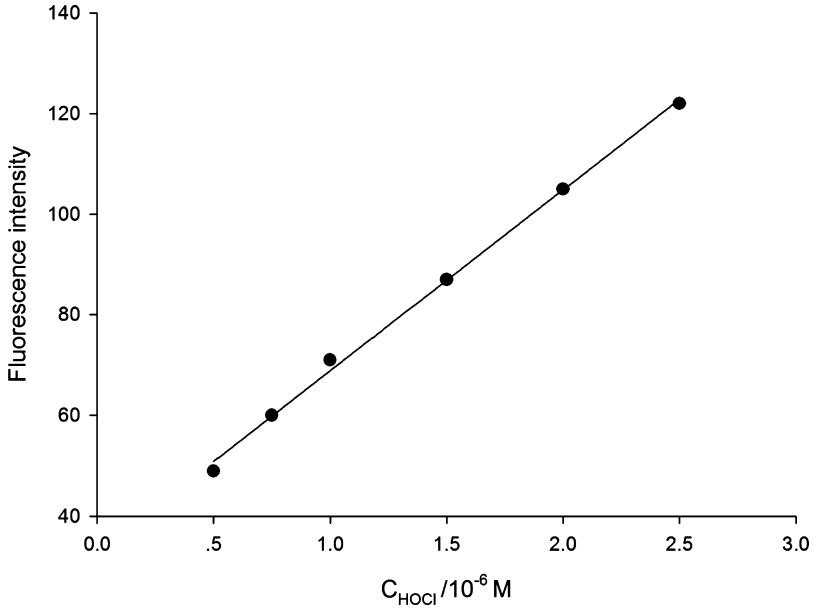


**Figure 2.** Fluorescence intensity changes of probe **1** (7.5 $\mu$M) as a dependence of the concentration of HClO in the range of 0.50 to 2.5 $\mu$M ($\lambda$em = 488 nm).

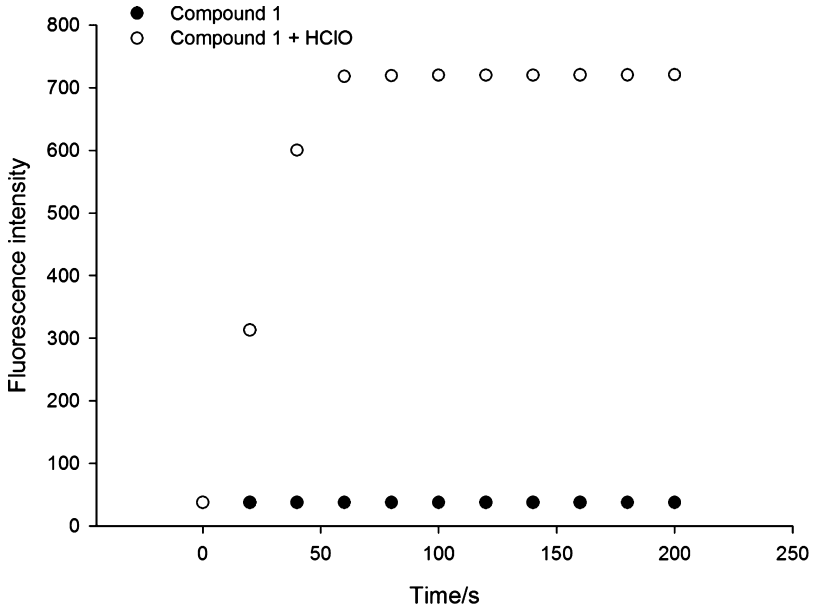


**Figure 3.** Time-dependent fluorescence intensity of probe **1** (7.5 $\mu$M) before (filled circles) and after adding 30 $\mu$M HClO (clear circles). Time points stand for 0, 20, 40, 60, 80, 100, 120, 140, 160, 180, and 200 s, $\lambda$ex = 370 nm and $\lambda$em = 488 nm.

## RESULTS AND DISCUSSION

**Spectroscopic Analytical Performance of Probe 1 toward HClO.** To investigate the fluorescence recognizing characteristics of the probe for HClO, we recorded the changes of the fluorescence sensing properties of the probe for various concentrations of HClO in buffered (0.01 mol·$L^{-1}$ PBS, pH = 7.40) aqueous acetonitrile solution (acetonitrile/water = 1:1, v/v) (Figure 1). As expected, when HClO is absent, the free probe showed weak fluorescence at 488 nm. After adding gradually increasing concentration of HClO, the fluorescence emission intensity at 488 nm was progressively enhanced to the maximum. These results establish the base for determining HClO concentration with probe **1** reported in the present work.

**Principle of Operation and the Basis of the Quantitative Assay.** In addition, to accurately quantify the concentration of the target, the linear relationship between the fluorescence intensity of the probe and the concentration of HClO was further studied (Figure 2). The linear dependence of the fluorescence intensity at 488 nm on HClO concentration was gained in the HClO concentration scope of $5.0 \times 10^{-7}$ to $2.5 \times 10^{-6}$ mol·$L^{-1}$. The linear regression equation was $F = 32.8912 + 35.9579 \times 10^6 \times C$ ($r = 0.9989$). In this equation, $F$ stands for the fluorescence intensity of probe **1** at 488 nm. $C$ denotes the concentration of HClO, and $r$ represents the linear correlation coefficient. The detection limit was calculated according to three-times standard deviation of blank solution.[42,47−50] The detection limit for



https://doi.org/10.1021/acsomega.1c01271
ACS Omega 2021, 6, 14399−14409

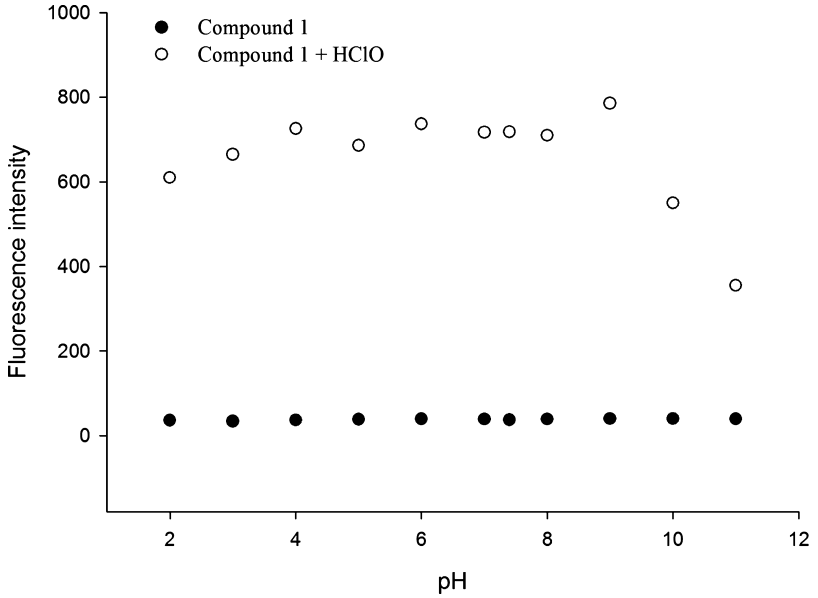


**Figure 4.** Influence of pH on the fluorescence emission intensity ($\lambda$em = 488 nm) of 7.5 $\mu$M probe **1** before (filled circles) and after adding 30 $\mu$M HClO (clear circles). The data were gained at different pH values (pH 2.00−11.00).

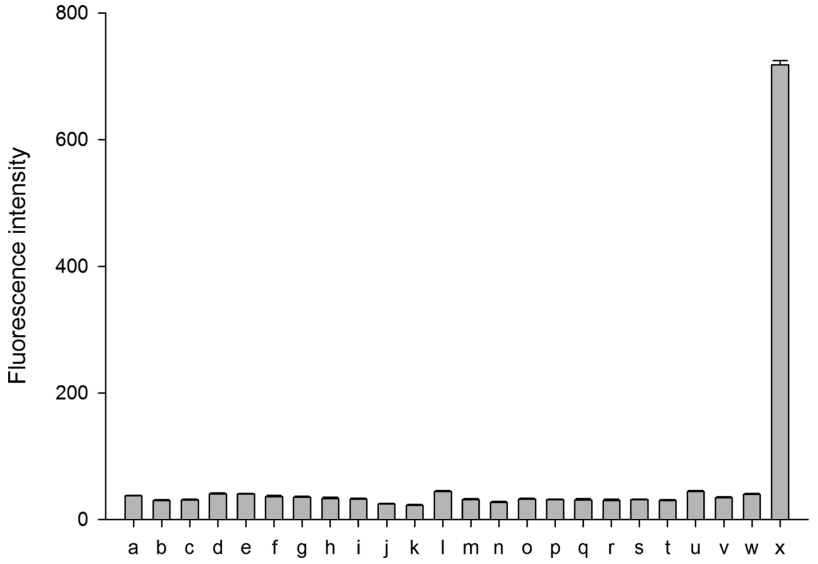


**Figure 5.** Fluorescence dependence of probe **1** (7.5 $\mu$M) on HClO (30 $\mu$M) and other different substances (500 $\mu$M except for specifically being labeled): (a) only probe, (b) $K^+$, (c) $Na^+$, (d) $Ca^{2+}$, (e) $Mg^{2+}$, (f) $Al^{3+}$, (g) $Zn^{2+}$, (h) $H_2O_2$, (i) TBHP, (j) $^{\bullet}OH$, (k) $^{\bullet}O^tBu$, (l) $^1O_2$, (m) ascorbic acid, (n) $O_2^{\bullet-}$, (o) $NO_3^-$, (p) $NO_2^-$, (q) Cys, (r) Hcy, (s) GSH, (t) $ONOO^-$, (u) $Fe^{2+}$, (v) $Fe^{3+}$, (w) $Cu^{2+}$ (100 $\mu$M), and (x) HClO.

HClO was 2.3 × $10^{-7}$ mol·$L^{-1}$. In comparison with other fluorescent probes for HClO located in mitochondria (as listed in Table S1),[51−55] this probe possessed the following superiority: low detection limit, fast response time, and powerful potential implement for imaging HClO in mitochondria. The results of this experiment indicated that the probe could be used as a highly sensitive fluorescence probe for quantitative detection of HClO.

**Time-Dependent Response of Probe 1 toward HClO.** The time-dependent fluorescence intensity changes of probe **1** for HClO were investigated by recording the variation of fluorescent intensity at 488 nm with the addition of HClO (30 $\mu$M) (Figure 3). As we can see from Figure 3, the fluorescent intensity emitted at 488 nm notably enhanced and achieved a plateau at around 60 s after adding 30 $\mu$M HClO. The experimental results indicated that probe **1** was steady under the assay conditions, and the detection of HClO could be finished within 60 s. In the present paper, an experimental time of 3 min was utilized as the optimal measurement condition.

**Effect of pH.** The pH scope suitable for HClO detection was studied (Figure 4). In the pH scope from 2.00 to 11.00, the fluorescence emission intensity of single probe **1** was quite stable, while the fluorescence intensity of the probe was significantly increased with treatment of HClO in the range of pH 2.00−11.00. The fluorescence intensity of the probe decreased from pH 9.00 to pH 11.00. The result demonstrated that the probe sensed HClO instead of $ClO^-$. The experimental results displayed that probe **1** had the excellent response to HClO in the range of pH 2.00−11.00. This pH scope covers the pH of physiological environment, demonstrating that probe **1** could have excellent sensing ability in vivo and accurately detect HClO in living cells.


https://doi.org/10.1021/acsomega.1c01271
ACS Omega 2021, 6, 14399−14409

**Selectivity.** To determine the role of probe **1** to selectively sense HClO, the fluorescence dependence of probe **1** on the latent interfering substances including ROS, RNS, and metal ions was investigated (Figure 5). Upon adding other interfering substances, the fluorescence intensity ($\lambda$em = 488 nm) of probe **1** did not obviously change. Only upon adding HClO, the fluorescence intensity ($\lambda$em = 488 nm) of probe **1** was greatly enhanced. This result suggested that the probe **1** has superior selectivity for HClO.

**Proposed Mechanism.** According to previous reports,[42,46] we speculated that the fluorescence enhancement of probe **1** was the result of intramolecular cyclization of the thiourea group of probe **1** with HClO to yield compound **5** (Scheme 2). The synthesis and characterization of compound **5** are

**Scheme 2. Probable Sensing Mechanism of Probe 1 for HClO**

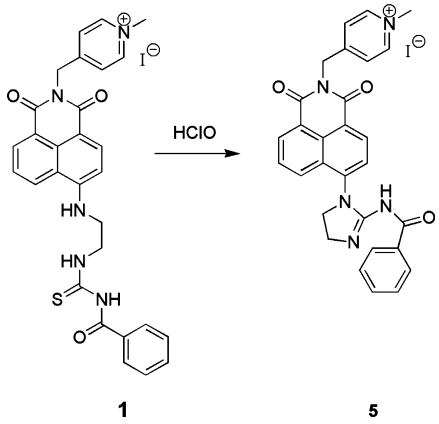


listed in the Supporting Information. $^1$H NMR, $^{13}$C NMR, and MS of compound **5** are displayed in Figures S1, S2, and S3 in the Supporting Information. With the aim of verifying the sensing mechanism of the probe to HClO, we studied probe **1**, the coexistence of probe **1**, HClO and compound **5** by UV−visible absorption spectroscopy and high-performance liquid chromatography (HPLC). As we can see from Figure 6, free probe **1** displayed the maximum absorption peak of 451 nm and compound **5** had strong absorption at 363 nm. When HClO was added, the maximum absorption wavelength of the probe moved from 451 to 363 nm, which was the same as the maximum absorption wavelength of compound **5**. In addition, the color of probe **1** solution varied from yellow to colorless. The result explained that the response of the probe **1** with HClO probably yielded the compound **5**. To further verify the proposed mechanism, HPLC experiments were carried out. As exhibited in Figure 7, the retention time of the probe alone was 13.70 min. It was satisfactory that the mixture of the probe and HClO had a peak at 5.15 min, and the retention time of the peak was almost the same as that of the single compound **5**. This result further indicated that the new compound in the coexistence of probe **1** and HClO was compound **5**. Furthermore, the response product of the probe and HClO was refined and characterized by $^1$H NMR, $^{13}$C NMR, and MS. $^1$H NMR (500 MHz, DMSO-$d_6$), $\delta$(ppm): 9.44 (1H, s), 8.87 (2H, d, $J$ = 6.6 Hz), 8.59−8.55 (3H, m), 8.18 (2H, d, $J$ = 6.6 Hz), 7.98 (1H, d, $J$ = 7.9 Hz), 7.90−7.87 (1H, m), 7.63 (1H, d, $J$ = 7.2 Hz), 7.34 (1H, t, $J$ = 7.4 Hz), 7.18 (2H, t, $J$ = 7.5 Hz), 5.51 (2H, s), 4.29 (3H, s), 4.14−4.09 (2H, m), 3.94 (2H, t, $J$ = 8.4 Hz) (Figure S4, Supporting Information). $^{13}$C NMR

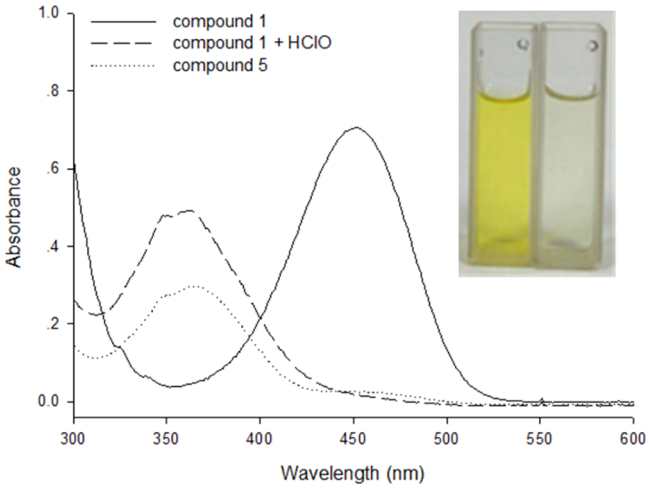


**Figure 6.** Absorption spectra of fluorescent probe **1** ($3.75 \times 10^{-5}$ M), compound **5** ($3.75 \times 10^{-5}$ M), and the reaction product of fluorescent probe **1** ($3.75 \times 10^{-5}$ M) with HClO ($1.0 \times 10^{-3}$ M). The solid line (−), dotted line (···), and medium dash (—) stand for fluorescent probe **1**, compound **5**, and the reaction product of fluorescent probe **1** with HClO, separately. Inset: color variations of probe **1** before and after adding HClO.

(125 MHz, DMSO-$d_6$), $\delta$(ppm):175.24, 163.74, 163.26, 162.08, 156.81, 145.18, 143.19, 137.75, 131.62, 131.30, 131.14, 131.02, 128.92, 128.55, 128.33, 127.67, 126.84, 125.26, 124.61, 122.47, 120.62, 48.59, 47.33, 42.85, 41.62 (Figure S5, Supporting Information). MS (ESI) $m/z$: $[M - I]^+$ 490.1873, $[M - I + H_2O]^+$ 508.1973 (Figure S6, Supporting Information). $^1$H NMR, $^{13}$C NMR and MS of the yielding product are practically the same as that of the accurate compound **5**.

**Cytotoxicity Assays and Confocal Imaging in Living Cells.** The cell cytotoxicity is an important factor to evaluate the performance of the probe. The 3-(4, 5-dimethylthiazole-2)-2, 5-diphenyltetrazolium bromide (MTT) assay was utilized to measure the cell cytotoxicity. As shown in Figure 8, when PC-12 cells were cultured with various concentrations of probe **1** and compound **5**, higher than 90% was obtained for the survival rate. The results showed that probe **1** and compound **5** had almost no cytotoxicity. First, control images of MitoTracker only (without compound **1**) in both the blue and red channels have been studied before and after adding 20 $\mu$M HClO (Figure S7, Supporting Information). From Figure S7, we can see that the mitochondrial depolarization did not occur in the presence of 20 $\mu$M HClO. Then, in order to quantify the spectral crosstalk of the dye in the red channel, control images of compound **1** in the absence of MitoTracker in both the blue and red channels were investigated before and after adding 20 $\mu$M HClO (Figure S8, Supporting Information). The experimental results of Figure S8 demonstrated that the spectral crosstalk of the probe did not exist in the red channel. Next, laser confocal fluorescence imaging was applied to record the probe's capability to monitor HClO in mitochondria (Figure 9). As shown in Figure 9b, PC-12 cells were incubated in the medium including 5 $\mu$M probe **1** and 1 $\mu$M Mito-Tracker Red CMXRos for 30 min, and very weak blue fluorescence was observed in the blue channel. However, strong blue fluorescence was observed in the blue channel in the control group (Figure 9e). The results demonstrated that probe was able to determine HClO in living cells. Then, we


https://doi.org/10.1021/acsomega.1c01271
ACS Omega 2021, 6, 14399−14409

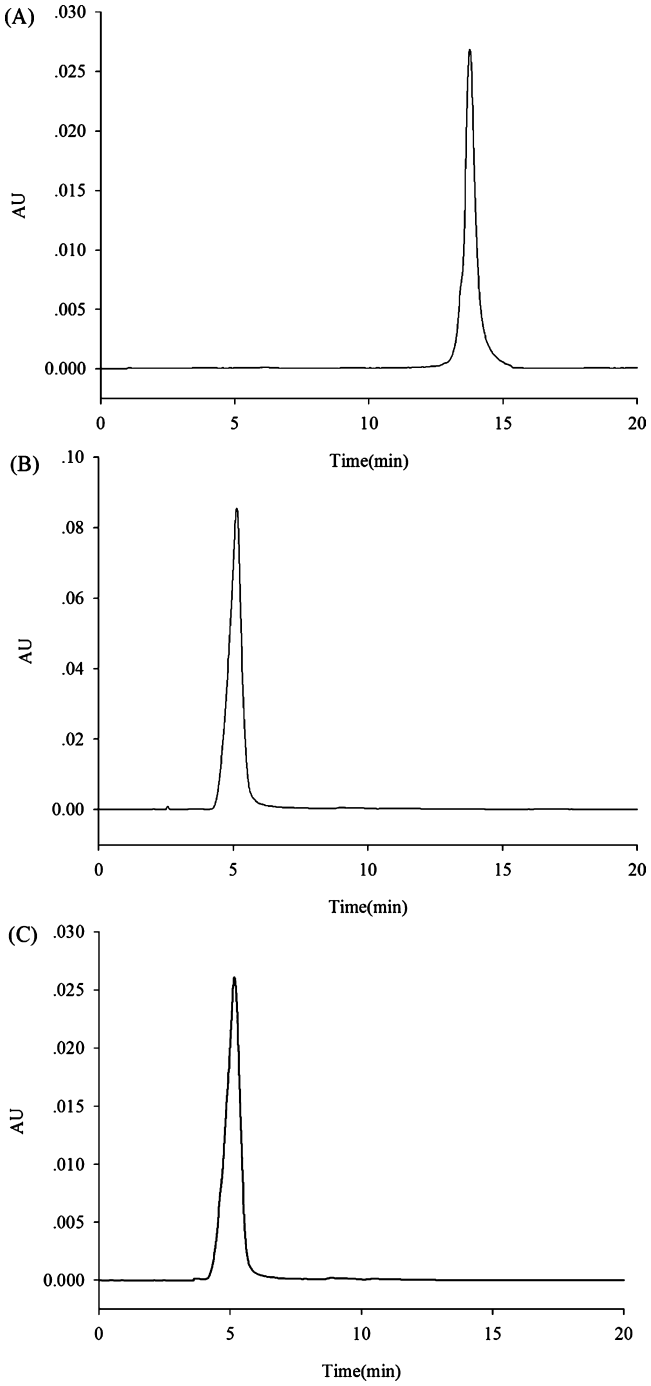


**Figure 7.** HPLC profiles of (A) compound **1** ($2.5 \times 10^{-4}$ M), (B) reaction product of compound **1** ($2.5 \times 10^{-4}$ M) with HClO ($5.0 \times 10^{-4}$ M) and (C) compound **5** ($2.5 \times 10^{-4}$ M). HPLC conditions: total flow rate is 1.0 mL·min$^{-1}$, the column is Agela Technologies Venusil XBP $-C_{18}$ (5 $\mu$m, 4.6 × 250 mm), the elution system is methanol/water = 35:65 (v/v), and the detection wavelength is 380 nm.

also confirm if the probe has the capability to target the mitochondria. The blue fluorescence image (Figure 9e) was overlaid with the red fluorescence image (Figure 9g) shown by MitoTracker Red CMXRos, and the Pearson's correlation coefficient reached 0.79. Finally, probe **1** was applied to detect endogenous HClO (Figure S9, Supporting Information). As displayed in Figure S9, RAW 264.7 cells cultured with only probe **1** displayed negligible intracellular fluorescence (Figure S9b). When RAW 264.7 cells were stimulated with phorbol myristate acetate (PMA) (1.5 $\mu$g/mL) for 30 min and then cultured with 5.0 $\mu$M compound **1** for 30 min, remarkable blue fluorescence was observed (Figure S9b). Thus, the probe could be applied as a mitochondria-targeting fluorescence probe for determining HClO.

## CONCLUSIONS

In conclusion, a novel mitochondria-specific and naphthalimide-based fluorescent probe for detecting HClO was designed and synthesized. (2-Aminoethyl)-thiourea was used as a sensing unit, and the quaternized pyridinium moiety was applied as a mitochondria-targeted unit. When HClO is absent, the developed probe exhibited weak fluorescence. Upon adding HClO, a strong blue fluorescence was seen. The probe possessed high selectivity and excellent sensitivity for HClO, and the detection limit was estimated to be $2.3 \times 10^{-7}$ mol·L$^{-1}$. Moreover, the turn-on probe owned the ability to target mitochondria of PC-12 cells. The probe had been efficaciously used to determine HClO in mitochondria of PC-12 cells.

## EXPERIMENTAL SECTION

**Materials and Instruments.** 4-Bromo-1,8-naphthalenic anhydride and 4-pyridylethylamine were gained from Saen Chemical Technology (Shanghai) Company. Benzoyl isothiocyanate was obtained from Tianjin Heowns Biochemical Technology Company. Ethylenediamine and dimethylsulfoxide (DMSO) were purchased from Tianjin Kaitong Chemical Reagent Company. The chromatographic pure solvents were used in the HPLC experiments and gained from Tianjin Siyou Fine Chemical Company. Cysteine (Cys) and homocysteine (Hys) were purchased from TCI (Shanghai) Development Company. Glutathione (GSH) was obtained from Aladdin Reagent Company. Sodium hypochlorite was supplied by Tianjin Fuyu Fine Chemical Company. Hydrogen peroxide ($H_2O_2$) was gained from 30% aqueous solutions. *tert*-Butyl hydroperoxide (TBHP) was obtained from 70% aqueous solutions. PMA was supplied by Beyotime Biotechnology Company. The reaction between 1 mM $Fe^{2+}$ with 200 $\mu$M $H_2O_2$ was utilized to produce the hydroxyl radical ($^{\bullet}OH$). *tert*-Butoxy radical ($^{\bullet}O^{t}Bu$) was yielded by the reaction between 1 mM $Fe^{2+}$ with 200 $\mu$M TBHP. The potassium superoxide ($KO_2$) solid was used to produce superoxide ($O_2^{\bullet-}$) by diluting in DMSO. The interaction between 1 mM $ClO^-$ with 200 $\mu$M $H_2O_2$ was applied to obtain singlet oxygen ($^1O_2$). The interaction between $H_2O_2$ and $NaNO_2$ was utilized to produce peroxynitrite ($ONOO^-$). The concentration of $ONOO^-$ was determined from absorbance at 302 nm ($\varepsilon$ = 1670 L·mol$^{-1}$·cm$^{-1}$).[37] Anhydrous dichloromethane was collected by refluxing in $CaH_2$. Silica gel for column chromatography is of 200−300 mesh and purchased from Qingdao Haiyang Chemicals Company. An SZ-93 automatic double pure water distiller was utilized to purify water, and the purified water was further applied to prepare all aqueous solutions. Unless otherwise specified, all other chemical reagents applied in the present work were of analytical grade and were obtained from commercial suppliers. HClO was standardized at pH 12 ($\varepsilon_{292\ nm}$ = 350 L·mol$^{-1}$·cm$^{-1}$).[56]

A Bruker DRX-500 NMR spectrometer was used to record $^1$H NMR and $^{13}$C NMR spectra and tetramethylsilane (TMS) was applied as the internal standard. An Agilent Technologies


https://doi.org/10.1021/acsomega.1c01271
ACS Omega 2021, 6, 14399−14409

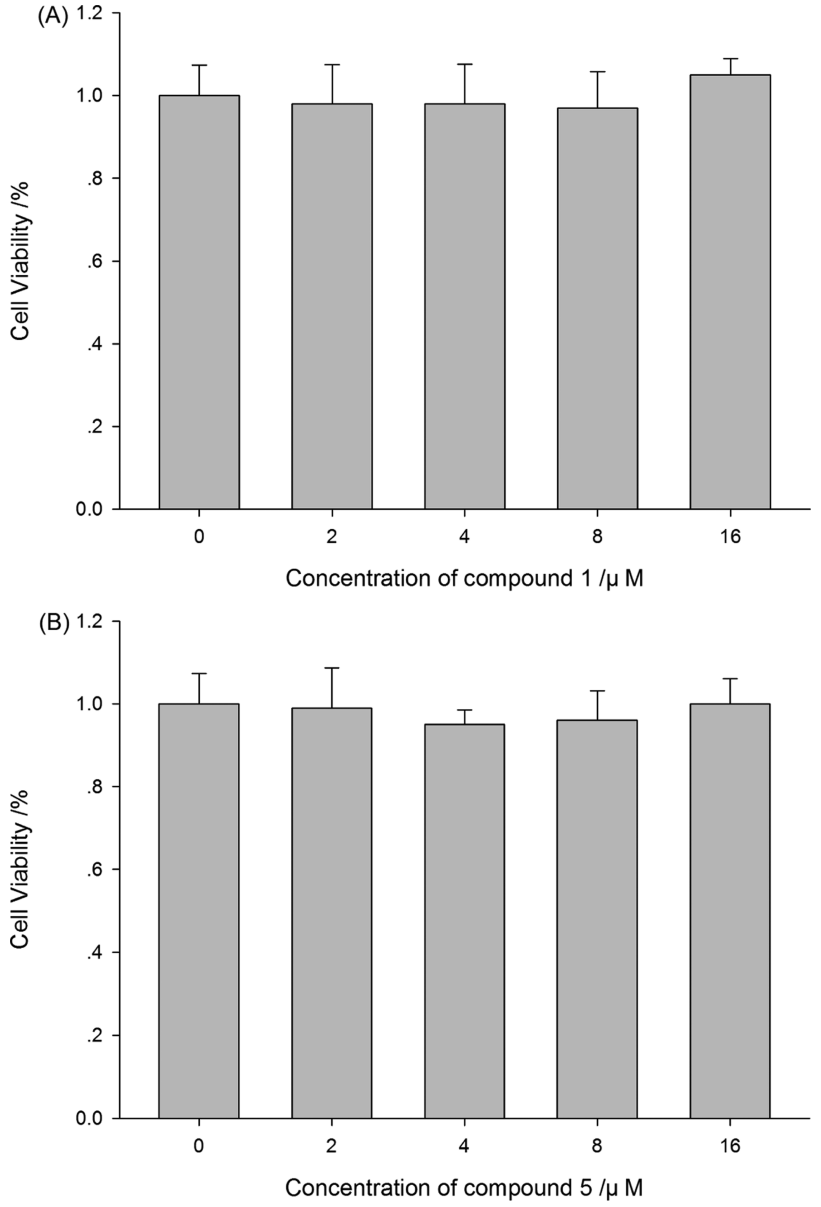


**Figure 8.** MTT assay of PC-12 cells upon adding various concentrations of compound **1** (A) and compound **5** (B) (0, 2, 4, 8, and 16 $\mu$M) for 24 h at 37 °C, respectively.

6420 Triple Quad LC/MS high-resolution mass spectrometer was utilized to measure the mass spectra. A Hitachi F-7000 fluorescence spectrophotometer was applied to measure fluorescence spectra, which has a 1 cm quartz absorption cell. An EVOLUTION 260 BIO spectrophotometer was utilized to record UV−visible absorption spectra, which has a 1 cm quartz absorption cell. A METTLER TOLEDO pH meter was used to measure the pH value. A Waters LC 2695−2998 HPLC/UV instrument with an XBP-$C_{18}$ column (5 $\mu$m, 4.6 × 250 mm) was applied to perform HPLC. An Olympus FV-1200 single-photon laser confocal microscope was used to record fluorescence imaging of living cells. In the fluorescence test, the samples were excited at 370 nm, the voltage of the photomultiplier tube was 400 V, and the entrance and exit slit width were both 5 nm. The buffered (0.01 mol·$L^{-1}$ PBS, pH = 7.40) aqueous acetonitrile solution (acetonitrile/water = 1:1, v/v) at room temperature was used to gain the data of fluorescence spectrophotometry and UV−visible spectrophotometry. Except for the fluorescence data recorded by time scanning, all other fluorescence and absorption data were measured at 3 min after adding HClO at room temperature.

**Syntheses.** The synthetic routes for fluorescence probe **1** are demonstrated in Scheme 1.

*Synthesis of Compound* ***2***. 4-Bromo-1,8-naphthalenic anhydride (0.43 g, 1.5 mmol) and 4-pyridylethylamine (0.16 mL, 1.5 mmol) were added into tetrahydrofuran (40 mL) at room temperature for 6 h, and a large quantity of the precipitate was produced. The precipitate was acquired by suction filtration and cleaned with tetrahydrofuran (5 × 2 mL), a saturated aqueous solution of $K_2CO_3$ (5 × 2 mL), and water (5 × 2 mL) to yield pure off-white solid compound **2** (0.45 g, 79%). $^1$H NMR (500 MHz, DMSO-$d_6$), $\delta$(ppm): 8.52 (2H, d, $J$ = 4.1 Hz), 8.40−8.36 (1H, m), 8.03−7.91 (2H, m), 7.79−7.70 (2H, m), 7.42 (2H, s), 4.48 (2H, d, $J$ = 3.2 Hz) (Figure S10, Supporting Information). MS (ESI) $m/z$: 367.0073 [M +


https://doi.org/10.1021/acsomega.1c01271
ACS Omega 2021, 6, 14399−14409

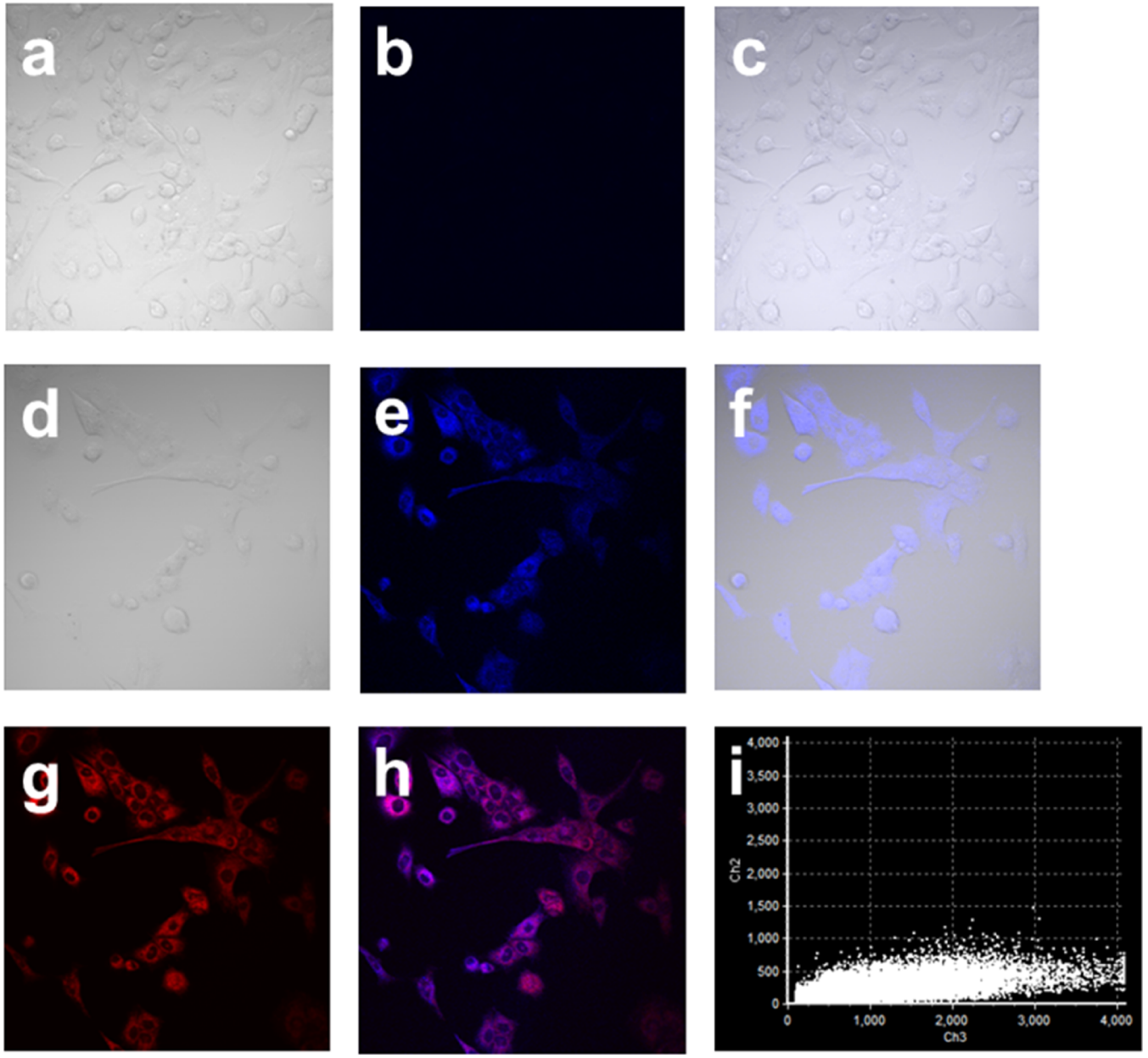


**Figure 9.** Images of PC-12 cells coincubated with probe **1** and MitoTracker Red CMXRos. (a) Bright-field transmission image of PC-12 cells cultured with 5.0 $\mu$M compound **1** and 1 $\mu$M MitoTracker Red CMXRos for 30 min; (b) fluorescence image from the blue channel of image (a); (c) overlay image of (a,b); (d) bright-field transmission image of PC-12 cells cultured with 5.0 $\mu$M compound **1** and 1 $\mu$M MitoTracker Red CMXRos for 30 min and then cultured with 20 $\mu$M HClO for 30 min; (e) fluorescence image from the blue channel of image (d); (f) overlay image of (d,e); (g) fluorescence image from the red channel of image (d); (h) overlay image of (e,g); (i) intensity correlation plot of (e,g).

$H]^+$, 369.0049 $[M + 2 + H]^+$ (Figure S11, Supporting Information).

*Synthesis of Compound* ***3***. Compound **2** (0.37 g, 1 mmol) and ethylenediamine (0.7 mL) were refluxed in ethylene glycol monomethyl ether (30 mL) for 4 h. The solution was concentrated to 5 mL under reduced pressure. A large amount of precipitates were precipitated by adding an appropriate amount of double-distilled water. The precipitates were gained by separation and recrystallized with 15 mL of chlorobenzene to afford compound **3** (0.21 g, 60%). $^1$H NMR (500 MHz, DMSO-$d_6$), $\delta$(ppm): 8.74 (1H, d, $J$ = 8.1 Hz), 8.46−8.43 (3H, m), 8.26 (1H, d, $J$ = 8.1 Hz), 7.68 (1H, t, $J$ = 7.4 Hz), 7.25 (2H, d, $J$ = 5.1 Hz), 6.82 (1H, d, $J$ = 8.2 Hz), 5.22 (2H, s), 3.39 (2H, t, $J$ = 6.4 Hz), 2.87 (2H, t, $J$ = 6.4 Hz) (Figure S12, Supporting Information). MS (ESI) $m/z$: 347.1497 $[M + H]^+$ (Figure S13, Supporting Information).

*Synthesis of Compound* ***4***. Compound **3** (0.35 g, 1 mmol) was treated with anhydrous dichloromethane (25 mL) under nitrogen, and then, benzoyl isothiocyanate (0.18 g, 1.1 mmol) was added dropwise. The mixture solution was stirred for 6 h at room temperature and then dried under reduced pressure. The residue was purified by column chromatography on silica gel with $CH_2Cl_2/CH_3OH$ (8:1, v/v) to provide compound **4** (0.24 g, 47%). $^1$H NMR (500 MHz, DMSO-$d_6$), $\delta$(ppm): 11.36 (1H, s), 11.06 (1H, s), 8.73 (1H, d, $J$ = 8.2 Hz), 8.45 (2H, d, $J$ = 5.5 Hz), 8.28 (1H, d, $J$ = 8.4 Hz), 8.01 (1H, s), 7.88 (2H, d, $J$ = 7.5 Hz), 7.74−7.71 (1H, m), 7.63−7.60 (1H, m), 7.49 (2H, t, $J$ = 7.4 Hz), 7.25 (2H, d, $J$ = 4.3 Hz), 7.04


https://doi.org/10.1021/acsomega.1c01271
ACS Omega 2021, 6, 14399−14409

(1H, d, $J$ = 8.5 Hz), 5.22 (2H, s), 4.02 (2H, d, $J$ = 5.8 Hz), 3.72 (2H, d, $J$ = 4.7 Hz) (Figure S14, Supporting Information). MS (ESI) $m/z$: 510.1588 $[M + H]^+$ (Figure S15, Supporting Information).

*Synthesis of Compound 1.* Compound **4** (0.51 g, 1 mmol) was dissolved in toluene and iodomethane (7.81 g, 55 mmol) was slowly added. The mixed solution was stirred for 2 h at room temperature and then refluxed for 3 h. The solvent was evaporated under reduced pressure, and the crude product was purified by silica column chromatography with $CH_2Cl_2$/$CH_3OH$ (6:1, v/v) to yield compound **1** (0.20 g, 31%). $^1H$ NMR (500 MHz, DMSO-$d_6$), $\delta$ (ppm): 11.37 (1H, s), 11.07 (1H, t, $J$ = 5.7 Hz), 8.83 (2H, d, $J$ = 6.6 Hz), 8.77 (1H, d, $J$ = 8.5 Hz), 8.46 (1H, d, $J$ = 7.3 Hz), 8.28 (1H, d, $J$ = 8.5 Hz), 8.07 (1H, t, $J$ = 5.2 Hz), 8.03 (2H, d, $J$ = 6.5 Hz), 7.89 (2H, d, $J$ = 7.6 Hz), 7.74 (1H, t, $J$ = 7.9 Hz), 7.62 (1H, t, $J$ = 7.3 Hz), 7.50 (2H, t, $J$ = 7.7 Hz), 7.06 (1H, d, $J$ = 8.7 Hz), 5.44 (2H, s), 4.27 (3H, s), 4.03 (2H, q, $J$ = 6.1 Hz), 3.73 (2H, q, $J$ = 5.9 Hz) (Figure S16, Supporting Information). $^{13}C$ NMR (125 MHz, DMSO-$d_6$), $\delta$(ppm): 180.77, 167.81, 163.93, 162.82, 157.28, 151.15, 145.19, 134.55, 132.97, 132.17, 131.11, 129.84, 129.13, 128.49, 128.40, 125.22, 124.53, 121.67, 120.34, 107.60, 104.35, 47.31, 43.05, 42.36, 41.14 (Figure S17, Supporting Information). MS (ESI) $m/z$: 524.1740 $[M\text{-}I]^+$ (Figure S18, Supporting Information).

**Cytotoxicity Assay.** For estimating the cytotoxicity of the probe, the MTT assay was applied to measure the cytotoxicity. First, PC-12 cells were incubated in 1640 medium. The 1640 medium used contained 10% fetal bovine serum, 100 units × $mL^{-1}$ penicillin, and 100 $\mu g \times mL^{-1}$ streptomycin. The cells in the logarithmic growth phase were seeded on a 96-well plate, with around $1 \times 10^4$ cells in each well, and the total volume of each well was 100 $\mu$L. The cells were incubated in an incubator containing 5% $CO_2$ for 24 h. The medium was removed and cleaned with Dulbecco's phosphate buffered saline (DPBS) three times. Then, probe **1** (0, 2, 4, 8, and 16 $\mu$M) and the purified product of compound **1** with HClO (0, 2, 4, 8, and 16 $\mu$M) were added, separately. After 4 h, the cells were sucked out of the medium containing drugs and then washed with DPBS and incubated in fresh 1640 medium for 24 h. Subsequently, the cells were incubated with 5 $mg{\cdot}mL^{-1}$ MTT (10 $\mu$L per well) for 4 h to guarantee the formation of formazan. At last, the above loading media was moved, followed by 150 $\mu$L of DMSO. The 96-well plates were vibrated for 10 min. A microplate reader was used to record the absorbance at 490 nm, and survival rate was estimated according to $A/A_0 \times 100\%$ ($A$ and $A_0$ are the absorbances of the experimental group and control group, respectively).

**Confocal Imaging in Living Cells.** In the experiment of cell imaging, PC-12 cells were incubated in a medium including 5 $\mu$M fluorescent probe **1** and 1 $\mu$M Mito-Tracker Red CMXRos at 37 °C for 30 min and then cleaned with DPBS three times. In the control experiment, the medium containing 5 $\mu$M probe was used to incubate PC-12 cells for 30 min at 37 °C, and the supernatant was sucked out. After cleaning with DPBS, PC-12 cells were incubated with the culture medium containing 50 $\mu$M HClO for another 30 min. DPBS was utilized to wash PC-12 cells for times for imaging. In order to confirm that fluorescent probe **1** has the ability to track mitochondrial HClO, 405 nm was selected as the excitation wavelength of blue channel and 594 nm was selected as the excitation wavelength of the red channel. The fluorescence imaging of cells was observed by an Olympus FV1200-MPE single photon confocal inverted microscope with a 40× objective lens.

## ■ ASSOCIATED CONTENT

### Supporting Information

The Supporting Information is available free of charge at https://pubs.acs.org/doi/10.1021/acsomega.1c01271.

$^1H$ and $^{13}C$ NMR spectra of compounds **1**−**5** and ESI-MS spectra of compounds **1**−**5** (PDF)

## ■ AUTHOR INFORMATION


### Corresponding Authors

**Qiujuan Ma** − *School of Pharmacy, Henan University of Traditional Chinese Medicine, Zhengzhou 450046, PR China*; orcid.org/0000-0001-9785-2733; Email: maqiujuan104@126.com

**Hongtao Zhang** − *Department of Dynamical Engineering, North China University of Water Resources and Electric Power, Zhengzhou 450011, PR China*; Email: 39583633@qq.com

**Baiyan Wang** − *Key Discipline Laboratory of Basic Medicine, Henan University of Traditional Chinese Medicine, Zhengzhou 450046, PR China*; Phone: +86-371-65676656; Email: 787354561@qq.com; Fax: +86-371-65680028

### Authors

**Junhong Xu** − *Department of Dynamical Engineering, North China University of Water Resources and Electric Power, Zhengzhou 450011, PR China*

**Chunyan Wang** − *School of Pharmacy, Henan University of Traditional Chinese Medicine, Zhengzhou 450046, PR China*

**Meiju Tian** − *School of Pharmacy, Henan University of Traditional Chinese Medicine, Zhengzhou 450046, PR China*

**Jingguo Sun** − *School of Pharmacy, Henan University of Traditional Chinese Medicine, Zhengzhou 450046, PR China*

**Yacong Chen** − *School of Pharmacy, Henan University of Traditional Chinese Medicine, Zhengzhou 450046, PR China*

Complete contact information is available at: https://pubs.acs.org/10.1021/acsomega.1c01271


### Notes

The authors declare no competing financial interest.

## ■ ACKNOWLEDGMENTS

This work was supported by the National Natural Science Foundation of China (grant nos. 21807027 and 31671580), the Zhongjing Scholars Research Funding of the Henan University of Chinese Medicine, the Graduate Innovation Fund of the Henan College of Chinese Medicine (2019KYCX031), and the Undergraduate Innovation Fund of the Henan College of Chinese Medicine (YXCX(2020)3).

## ■ REFERENCES

(1) Yap, Y. W.; Whiteman, M.; Bay, B. H.; Li, Y.; Sheu, F.-S.; Qi, R. Z.; Tan, C. H.; Cheung, N. S. Hypochlorous acid induces apoptosis of cultured cortical neurons through activation of calpains and rupture of lysosomes. *J. Neurochem.* **2006**, *98*, 1597−1609.

(2) Winterbourn, C. C. Reconciling the chemistry and biology of reactive oxygen species. *Nat. Chem. Biol.* **2008**, *4*, 278−286.

(3) Steinbeck, M. J.; Nesti, L. J.; Sharkey, P. F.; Parvizi, J. Myeloperoxidase and chlorinated peptides in osteoarthritis: potential biomarkers of the disease. *J. Orthop. Res.* **2007**, *25*, 1128−1135.

(4) Yap, Y. W.; Whiteman, M.; Cheung, N. S. Chlorinative stress: an under appreciated mediator of neurodegeneration? *Cell. Signal.* **2007**, *19*, 219−228.
(5) Prokopowicz, Z. M.; Arce, F.; Biedron, R.; Chiang, C. L.-L.; Ciszek, M.; Katz, D. R.; Nowakowska, M.; Zapotoczny, S.; Marcinkiewicz, J.; Chain, B. M.; Chain, B. M. Hypochlorous acid: a natural adjuvant that facilitates antigen processing, cross-priming, and the induction of adaptive immunity. *J. Immunol.* **2010**, *184*, 824−835.
(6) Roos, D.; Winterbourn, C. C. Immunology. Lethal weaponsIMMUNOLOGY: Enhanced: Lethal Weapons. *Science* **2002**, *296*, 669−671.
(7) Fang, F. C. Antimicrobial reactive oxygen and nitrogen species: concepts and controversies. *Nat. Rev. Microbiol.* **2004**, *2*, 820−832.
(8) Hammerschmidt, S.; Büchler, N.; Wahn, H. Tissue lipid peroxidation and reduced glutathione depletion in hypochlorite-induced lung injury. *Chest* **2002**, *121*, 573−581.
(9) Hazell, L. J.; Arnold, L.; Flowers, D.; Waeg, G.; Malle, E.; Stocker, R. Presence of hypochlorite-modified proteins in human atherosclerotic lesions. *J. Clin. Invest.* **1996**, *97*, 1535−1544.
(10) Wu, S. M.; Pizzo, S. V. $\alpha$2-Macroglobulin from Rheumatoid Arthritis Synovial Fluid: Functional Analysis Defines a Role for Oxidation in Inflammation. *Arch. Biochem. Biophys.* **2001**, *391*, 119−126.
(11) Malle, E.; Buch, T.; Grone, H.-J. Myeloperoxidase in kidney disease. *Kidney Int.* **2003**, *64*, 1956−1967.
(12) Nogueira, V.; Hay, N. Molecular pathways: reactive oxygen species homeostasis in cancer cells and implications for cancer therapy. *Clin. Cancer Res.* **2013**, *19*, 4309−4314.
(13) St-Pierre, J.; Buckingham, J. A.; Roebuck, S. J.; Brand, M. D. Topology of superoxide production from different sites in the mitochondrial electron transport chain. *J. Biol. Chem.* **2002**, *277*, 44784−44790.
(14) McBride, H. M.; Neuspiel, M.; Wasiak, S. Mitochondria: more than just a powerhouse. *Curr. Biol.* **2006**, *16*, R551−R560.
(15) Liochev, S. I.; Fridovich, I. The effects of superoxide dismutase on H2O2 formation. *Free Radic. Biol. Med.* **2007**, *42*, 1465−1469.
(16) Turrens, J. F. Mitochondrial formation of reactive oxygen species. *J. Physiol.* **2003**, *552*, 335−344.
(17) Hoye, A. T.; Davoren, J. E.; Wipf, P.; Fink, M. P.; Kagan, V. E. Targeting mitochondria. *Acc. Chem. Res.* **2008**, *41*, 87−97.
(18) Deng, Y.; Feng, S.; Xia, Q.; Gong, S.; Feng, G. A novel reaction-based fluorescence probe for rapid imaging of HClO in live cells, animals, and injured liver tissues. *Talanta* **2020**, *215*, 120901.
(19) Jović, M.; Cortés-Salazar, F.; Lesch, A.; Amstutz, V.; Bi, H. Y.; Girault, H. H. Electrochemical detection of free chlorine at inkjet printed silver electrodes. *J. Electroanal. Chem.* **2015**, *756*, 171−178.
(20) Soldatkin, A. P.; Gorchkov, D. V.; Martelet, C.; Jaffrezic-Renault, N. New enzyme potentiometric sensor for hypochlorite species detection. *Sens. Actuators, B* **1997**, *43*, 99−104.
(21) Caldwell, T. E.; Foster, K. L.; Benter, T.; Langer, S.; Hemminger, J. C.; Finlayson-Pitts, B. J. Characterization of HOCl using atmospheric pressure ionization mass spectrometry. *J. Phys. Chem. A* **1999**, *103*, 8231−8238.
(22) Jerlich, A.; Pitt, A. R.; Schaur, R. J.; Spickett, C. M. Pathways of phospholipid oxidation by HOCl in human LDL detected by LC-MS. *Free Radic. Biol. Med.* **2000**, *28*, 673−682.
(23) Dietrich, A. M.; Ledder, T. D.; Gallagher, D. L.; Grabeel, M. N.; Hoehn, R. C. Determination of chlorite and chlorate in chlorinated and chloraminated drinking water by flow injection analysis and ion chromatography. *Anal. Chem.* **1992**, *64*, 496−502.
(24) Yue, X.; Wang, J.; Han, J.; Wang, B.; Song, X. A dual-ratiometric fluorescent probe for individual and continuous detection of H2S and HClO in living cells. *Chem. Commun.* **2020**, *56*, 2849−2852.
(25) Ding, H.-L.; Pu, Y.-Q.; Ye, D.-Y.; Dong, Z.-Y.; Yang, M.; Lü, C.-W.; An, Y. The design and synthesis of two imidazole fluorescent probes for the special recognition of HClO/NaHSO3 and their applications. *Anal. Methods* **2020**, *12*, 2476−2483.
(26) Ma, Q.; Wang, C.; Mao, G.; Tian, M.; Sun, J.; Feng, S. An endoplasmic reticulum-targeting and ratiometric fluorescent probe for hypochlorous acid in living cells based on a 1,8-naphthalimide derivative. *New J. Chem.* **2020**, *44*, 18389−18398.
(27) Wang, L.; Liu, J.; Zhang, H.; Guo, W. Discrimination between cancerous and normal cells/tissues enabled by a near-infrared fluorescent HClO probe. *Sens. Actuators, B* **2021**, *334*, 129602.
(28) Ma, Q.; Wang, C.; Bai, Y.; Xu, J.; Zhang, J.; Li, Z.; Guo, X. A lysosome-targetable and ratiometric fluorescent probe for hypochlorous acid in living cells based on a 1,8-naphthalimide derivative. *Spectrochim. Acta, Part A* **2019**, *223*, 117334.
(29) Mao, G.-J.; Wang, Y.-Y.; Dong, W.-P.; Meng, H.-M.; Wang, Q.-Q.; Luo, X.-F.; Li, Y.; Zhang, G. A lysosome-targetable two-photon excited near-infrared fluorescent probe for visualizing hypochlorous acid-involved arthritis and its treatment. *Spectrochim. Acta, Part A* **2021**, *249*, 119326.
(30) Zhang, P.; Wang, H.; Zhang, D.; Zeng, X.; Zeng, R.; Xiao, L.; Tao, H.; Long, Y.; Yi, P.; Chen, J. Two-photon fluorescent probe for lysosome-targetable hypochlorous acid detection within living cells. *Sens. Actuators, B* **2018**, *255*, 2223−2231.
(31) Zhang, P.; Wang, H.; Hong, Y.; Yu, M.; Zeng, R.; Long, Y.; Chen, J. Selective visualization of endogenous hypochlorous acid in zebrafish during lipopolysaccharide-induced acute liver injury using a polymer micelles-based ratiometric fluorescent probe. *Biosens. Bioelectron.* **2018**, *99*, 318−324.
(32) Xue, M.; Wang, H.; Chen, J.; Ren, J.; Chen, S.; Yang, H.; Zeng, R.; Long, Y.; Zhang, P. Ratiometric fluorescent sensing of endogenous hypochlorous acid in lysosomes using AIE-based polymeric nanoprobe. *Sens. Actuators, B* **2019**, *282*, 1−8.
(33) Huang, X.; Li, Z.; Liu, Z.; Zeng, C.; Hu, L. A near-infrared fluorescent probe for endogenous hydrogen peroxide real-time imaging in living cells and zebrafish. *Dyes Pigm.* **2019**, *165*, 518−523.
(34) Wang, C.; Wang, Y.; Wang, G.; Huang, C.; Jia, N. A new mitochondria-targeting fluorescent probe for ratiometric detection of H2O2 in live cells. *Anal. Chim. Acta* **2020**, *1097*, 230−237.
(35) Li, Z.; Ren, T.-B.; Zhang, X.-X.; Xu, S.; Gong, X.-Y.; Yang, Y.; Ke, G.; Yuan, L.; Zhang, X.-B. Precipitated fluorophore-based probe for accurate detection of mitochondrial analytes. *Anal. Chem.* **2021**, *93*, 2235−2243.
(36) Jiao, S.; Zhai, J.; Yang, S.; Meng, X. A highly responsive, sensitive NIR fluorescent probe for imaging of superoxide anion in mitochondria of oral cancer cells. *Talanta* **2021**, *222*, 121566.
(37) Deng, T.; Wang, X.; Wu, S.; Hu, S.; Liu, W.; Chen, T.; Yu, Z.; Xu, Q.; Liu, F. A new FRET probe for ratiometric fluorescence detecting mitochondria-localized drug activation and imaging endogenous hydroxyl radicals in zebrafish. *Chem. Commun.* **2020**, *56*, 4432−4435.
(38) Yuan, G.; Ding, H.; Sun, H.; Zhou, L.; Lin, Q. A mitochondrion-targeting turn-on fluorescent probe detection of endogenous hydroxyl radicals in living cells and zebrafish. *Sens. Actuators, B* **2019**, *296*, 126706.
(39) Li, M.-Y.; Li, K.; Liu, Y.-H.; Zhang, H.; Yu, K.-K.; Liu, X.; Yu, X.-Q. Mitochondria-immobilized fluorescent probe for the detection of hypochlorite in living cells, tissues, and zebrafishes. *Anal. Chem.* **2020**, *92*, 3262−3269.
(40) Teng, H.; Tian, J.; Sun, D.; Xiu, M.; Zhang, Y.; Qiang, X.; Tang, H.; Guo, Y. A mitochondria-specific fluorescent probe based on triazolopyridine formation for visualizing endogenous hypochlorous acid in living cells and zebrafish. *Sens. Actuators, B* **2020**, *319*, 128288.
(41) Gong, J.; Liu, C.; Cai, S.; He, S.; Zhao, L.; Zeng, X. Novel near-infrared fluorescent probe with a large Stokes shift for sensing hypochlorous acid in mitochondria. *Org. Biomol. Chem.* **2020**, *18*, 7656−7662.
(42) Mao, G.-J.; Gao, G.-Q.; Liang, Z.-Z.; Wang, Y.-Y.; Su, L.; Wang, Z.-X.; Zhang, H.; Ma, Q.-J.; Zhang, G. A mitochondria-targetable two-photon fluorescent probe with a far-red to near-infrared emission for sensing hypochlorite in biosystems. *Anal. Chim. Acta* **2019**, *1081*, 184−192.


https://doi.org/10.1021/acsomega.1c01271
*ACS Omega* 2021, 6, 14399−14409

(43) Wang, Q.-M.; Jin, L.; Shen, Z.-Y.; Xu, J.-H.; Sheng, L.-Q.; Bai, H. Mitochondria-targeting turn-on fluorescent probe for HClO detection and imaging in living cells. *Spectrochim. Acta Mol. Biomol. Spectrosc.* **2020**, *228*, 117825.
(44) Ning, P.; Wang, W.; Chen, M.; Feng, Y.; Meng, X. Recent advances in mitochondria- and lysosomes-targeted small-molecule two-photon fluorescent probes. *Chin. Chem. Lett.* **2017**, *28*, 1943−1951.
(45) Ren, M.; Zhou, K.; He, L.; Lin, W. Mitochondria and lysosome-targetable fluorescent probes for HOCl: recent advances and perspectives. *J. Mater. Chem. B* **2018**, *6*, 1716−1733.
(46) Shu, W.; Jia, P.; Chen, X.; Li, X.; Huo, Y.; Liu, F.; Wang, Z.; Liu, C.; Zhu, B.; Yan, L.; Du, B. A highly selective ratiometric fluorescent probe for the sensitive detection of hypochlorous acid and its bioimaging applications. *RSC Adv.* **2016**, *6*, 64315−64322.
(47) Xiong, J.; Zheng, T.-j.; Shi, Y.; Wei, F.; Ma, S.-c.; He, L.; Wang, S.-c.; Liu, X.-s. Analysis of the fingerprint profile of bioactive constituents of traditional Chinese medicinal materials derived from animal bile using the HPLC-ELSD and chemometric methods: an application of a reference scaleplate. *J. Pharm. Biomed. Anal.* **2019**, *174*, 50−56.
(48) Shen, Y.; Zhang, X.; Zhang, Y.; Li, H.; Chen, Y. An ICT-modulated strategy to construct colorimetric and ratiometric fluorescent sensor for mitochondria-targeted fluoride ion in cell living. *Sens. Actuators, B* **2018**, *258*, 544−549.
(49) Shen, Y.; Zhang, X.; Zhang, Y.; Wu, Y.; Zhang, C.; Chen, Y.; Jin, J.; Li, H. A mitochondria-targeted colorimetric and ratiometric fluorescent probe for hydrogen peroxide with a large emission shift and bio-imaging in living cells. *Sens. Actuators, B* **2018**, *255*, 42−48.
(50) Shen, Y.; Gu, B.; Liu, X.; Tang, Y.; Li, H. A benzothiazole-based ratiometric fluorescent probe for highly selective detection of homocysteine and its bioimaging application. *Chin. J. Org. Chem.* **2020**, *40*, 2442−2449.
(51) Cheng, G.; Fan, J.; Sun, W.; Sui, K.; Jin, X.; Wang, J.; Peng, X. A highly specific BODIPY-based probe localized in mitochondria for HClO imaging. *Analyst* **2013**, *138*, 6091−6096.
(52) Xiao, H.; Li, J.; Zhao, J.; Yin, G.; Quan, Y.; Wang, J.; Wang, R. A colorimetric and ratiometric fluorescent probe for ClO−targeting in mitochondria and its application in vivo. *J. Mater. Chem. B* **2015**, *3*, 1633−1638.
(53) Tian, F.; Jia, Y.; Zhang, Y.; Song, W.; Zhao, G.; Qu, Z.; Li, C.; Chen, Y.; Li, P. A HClO-specific near-infrared fluorescent probe for determination of myeloperoxidase activity and imaging mitochondrial HClO in living cells. *Biosens. Bioelectron.* **2016**, *86*, 68−74.
(54) Li, D.; Feng, Y.; Lin, J.; Chen, M.; Wang, S.; Wang, X.; Sheng, H.; Shao, Z.; Zhu, M.; Meng, X. A mitochondria-targeted two-photon fluorescent probe for highly selective and rapid detection of hypochlorite and its bio-imaging in living cells. *Sens. Actuators, B* **2016**, *222*, 483−491.
(55) Zheng, A.; Liu, H.; Peng, C.; Gao, X.; Xu, K.; Tang, B. A mitochondria-targeting near-infrared fluorescent probe for imaging hypochlorous acid in cells. *Talanta* **2021**, *226*, 122152.
(56) Morris, J. C. The Acid Ionization Constant of HOCl from 5 to 35°. *J. Phys. Chem.* **1966**, *70*, 3798−3805.


https://doi.org/10.1021/acsomega.1c01271
*ACS Omega* 2021, 6, 14399−14409